membranes made of natural polyesters.

The laminester is not soluble in organic solvents like chloroform or benzene, suggesting it has a very high molecular weight. It is so hydrophobic that a fine layer of air forms between the membrane and water. Further indication of its hydrophobicity is the fact that it is untouched by 12*N* aqueous HCl at 100°C overnight, but, as mentioned above, methanolic HCl at 100°C completely hydrolyzes it in 2 hours. Similarly, the polyester was unaffected by treatment with 60 percent aqueous KOH, but addition of methanol to the solution (50 percent by volume) resulted in rapid hydrolysis. These hydrophobic characteristics probably explain how these cell linings resist physical and biological attack and remain intact in soil for more than a year.

Although in ants the Dufour's gland produces secretions that serve as pheromones (*15*), the use of the Dufour's gland products for cell construction in Apoidea is unique. The production and utilization of the lactones provide the bees not only with an efficient protective membrane but also, because of their fragrance combined with the fragrance of the related aldehydes, might serve in nest location and recognition as suggested (*8*). The possible additional function of the lactones as pheromones was not investigated. However, Dufour's gland secretion of *Colletes* spp. retains its distinct musky fragrance for over a year, and the abdomens of actively nesting females smell strongly of these secretions.

ABRAHAM HEFETZ
HENRY M. FALES
Laboratory of Chemistry, National Heart, Lung, and Blood Institute, Bethesda, Maryland 20014
SUZANNE W. T. BATRA
Beneficial Insect Introduction Laboratory, Insect Identification and Beneficial Insect Introduction Institute, Science and Education Administration, Department of Agriculture, Beltsville, Maryland 20705

References and Notes

1. S. W. T. Batra, *J. Kans. Entomol. Soc.* **45**, 208 (1972) and references therein.
2. L. Dufour, *Ann. Soc. Entomol. Fr.* **4**, 594 (1835).
3. D. G. K. May, *J. Kans. Entomol. Soc.* **47**, 504 (1974).
4. E. de Lello, *ibid.* **44**, 5 (1971).
5. S. W. T. Batra, *Insectes Soc.* **11**, 159 (1964); *Ann. Entomol. Soc. Am.* **63**, 400 (1970).
6. G. Bergström, *Chem. Scripta* **5**, 39 (1974).
7. C. O. Andersson, G. Bergström, B. Kullenberg, S. Stollberg-Stenhagen, *Ark. Kemi* **26**, 191 (1966); A. Kefetz, M. S. Blum, G. C. Eickwort, J. W. Wheeler, *Comp. Biochem. Physiol.* **61B**, 129 (1978).
8. G. Bergström and J. Tengö, *Chem. Scripta* **5**, 28 (1974); J. Tengö and G. Bergström, *J. Chem. Ecol.* **1**, 253 (1975).
9. Bees were collected at their nesting site or on flowers in the vicinity of the nest. They were chilled on ice and dissected dry; the Dufour's gland was excised and then extracted with methylene chloride. The extracts were analyzed on an LKB-9000 combined GC-MS with a 25 m by 0.2 mm capillary SE-30 column. The chromatogram was programmed from 200° to 250°C at 10°C per minute. The lactones were identified by comparison to reported data (*6*, *7*).
10. F. Claude-Joseph (-H. Janvier), *Ann. Sci. Nat. Zool. Ser. 10* **9**, 113 (1926); H. Janvier, *ibid.* **16**, 209 (1933).
11. J. W. Hill and W. H. Carothers, *J. Am. Chem. Soc.* **55**, 5031 and 5039 (1933); E. W. Spanagel and W. H. Carothers, *ibid.* **58**, 654 (1936).
12. J. Pain, M. Barbier, D. Bogdanovsky, E. Lederer, *Comp. Biochem. Physiol.* **6**, 233 (1962).
13. E. von Rudloff, *Can. J. Chem.* **37**, 1038 (1959); J. Bougault and L. Bourdier, *Comp. Rend.* **147**, 1311 (1908).
14. We thank one of the referees for bringing to our attention the recent paper by G. Bergström and J. Tengö [*J. Chem. Ecol.* **4**, 437 (1978)] in which the possible polymerization of the hydroxy acids is mentioned.
15. M. S. Blum and J. M. Brand, *Am. Zool.* **12**, 553 (1972).

27 September 1978; revised 22 January 1979

Prolonged Inhibition of Neurons by Neuroendocrine Cells in *Aplysia*

Abstract. *In the abdominal ganglion of* Aplysia, *a burst of action potentials in peptide-secreting neuroendocrine cells, the bag cells, produces slow inhibition of two identified bursting pacemaker neurons. The inhibition is due to a slow hyperpolarizing potential that reduces bursting pacemaker activity for 3 hours or more. The slow inhibitory potential results from a large and prolonged increase in membrane conductance to potassium ions as well as a slower ionic process that is relatively independent of membrane conductance.*

The abdominal ganglion of the marine mollusk *Aplysia* is a convenient experimental system for investigating the roles of peptides as chemical messengers in the nervous system. The ganglion contains a group of neuroendocrine cells, the bag cells (1–4), that synthesize and secrete peptides (*5*). One of these is egg-laying hormone, a 6000-dalton peptide that induces egg laying (*6*). An electrically stimulated bag cell discharge produces prolonged augmentation of bursting pacemaker activity in R15, an identified neuron in the abdominal ganglion (*7*). The peptide is thought to mediate this interaction, since local application of the peptide duplicates the response (*8*). The response appears to be induced hormonally rather than transynaptically, for (i) it has a slow, smooth onset and (ii) there is no ultrastructural evidence for synaptic contacts between bag cell axons and other ganglion neurons.

The bag cell axons branch profusely in the sheath surrounding the ganglion, where they end near vascular spaces (Fig. 1A) (*3*). This distinctive anatomical arrangement led us to search for effects on other ganglion neurons (*9*). In this report we describe another type of bag cell action, prolonged inhibition, which lasts for 3 hours or more. Although this response may also be hormonally induced, the effect on electrical signaling and the ionic response mechanism resemble synaptically mediated slow inhibition.

Experiments were performed on abdominal ganglia isolated from sexually mature *Aplysia* (Pacific Biomarine, Venice, California) weighing 300 to 500 g. Animals were usually anesthetized by injecting 120 ml of isotonic $MgCl_2$ to prevent possible premature activation of the bag cells during dissection. The isolated ganglion was pinned to clear resin (Sylgard) in 33 percent isotonic $MgCl_2$ in artificial seawater (ASW) and washed for 30 minutes in ASW before experiments were begun. Experiments were conducted at 20°C in either perfused ASW or 15 ml of filtered standing blood taken from unanesthetized animals. Double-barreled microelectrodes filled with 4*M* potassium acetate were used for intracellular recordings and for passing current.

The bag cells are normally silent (*1*, *10*), but, after being locally stimulated with a brief 1- to 2-second train of electrical pulses (*11*), they fire in a burst of spike activity lasting approximately 20 minutes (*9*, *12*). Since they fire in near unison, their activity was monitored by an intracellular recording from one bag cell. A second intracellular electrode recorded the response of a target cell (Fig. 1A). The target cells are the identified bursting pacemaker neurons L_3 and L_6, which discharge in periodic bursts of action potentials (*4*). These cells lie adjacent to one another and respond identically to bag cell activity.

Figure 1B shows the first few minutes of slow inhibition following the onset of bag cell spike activity. Several seconds after the bag cells began to discharge, the target cell slowly hyperpolarized and all spiking was inhibited for 1 to 2 minutes. Thereafter, burst activity of the target cell resumed, but burst rate and average spike rate remained below baseline rates. The inhibition is due to a slow inhibitory potential (SIP) with an amplitude of 10 to 20 mV, which is superim-

0036-8075/79/0427-0417$00.50/0

posed on the ongoing bursting pacemaker activity of the cell. The effect of the SIP on membrane potential and impulse activity could be duplicated by applying a hyperpolarizing current through the second barrel of the microelectrode. During the bag cell discharge there was no sign of fast synaptic potentials in the target cell following individual bag cell spikes, nor other synaptic events that could account for the sustained hyperpolarization (Fig. 1B).

To determine whether the inhibition was contingent on bag cell activity, the bag cells of several ganglia were locally stimulated according to a fixed procedure that sometimes elicited a bag cell discharge. Inhibition, measured as the decrease in the mean spike rate of the target neuron, occurred only when bag cell discharges were evoked (Fig. 1C), even though there was no significant difference between intensities that did and did not evoke discharges. We therefore concluded that the inhibition was induced by the bag cell discharge.

The inhibition lasts at least 3 hours. In the experiment of Fig. 1C, mean spike rate of inhibited target cells was still 36 percent below the spike rate of unaffected cells after 2 hours. In other long-term recordings, inhibition lasted 3 hours or more.

We next studied the ionic mechanism of the SIP, limiting our investigation to the first 45 minutes of the response. At the onset of the response (Fig. 2A), the polarity of the SIP was inverted when the target cell was hyperpolarized to −122 mV by constant current injection. This finding suggests that the SIP results from an increase in membrane conductance to one or more ions. The onset of the inverted response, like the normal SIP of unpolarized cells, was slow and smoothly graded and not associated with an altered pattern of synaptic inputs from other neurons (*13*).

The reversal potential of the SIP indicates the equilibrium potential for the ion that produces the SIP. The usual procedure for determining reversal potential is to elicit a response repeatedly, each time at a different level of imposed membrane current. This procedure was precluded, however, by the prolonged duration of the SIP. To avoid this difficulty, a single SIP was elicited, and, at regular intervals, the membrane potential response to three levels of imposed hyperpolarizing current was determined. Responses were measured at 2.33-minute intervals to a three-step current pulse lasting 14 seconds (Fig. 2B). The steady-state membrane potential recorded at the end of each step of current was then plotted as a function of time (Fig. 2C). To simplify the description of these results, we shall discuss the changes occurring in the first minute of the SIP (the early phase) separately from those occurring later (the late phase). The early phase is considered first.

The SIP typically reached a peak hyperpolarization several tens of seconds after onset of the bag cell burst (*14*). In the example shown, the peak occurred at 0.70 minute. At this time there was no change in the membrane potential (−84 mV) produced by the first level of hyperpolarizing current (−15 nA), compared with the baseline value. For the second and third levels of current (−24.2 and −32.6 nA), however, the membrane po-

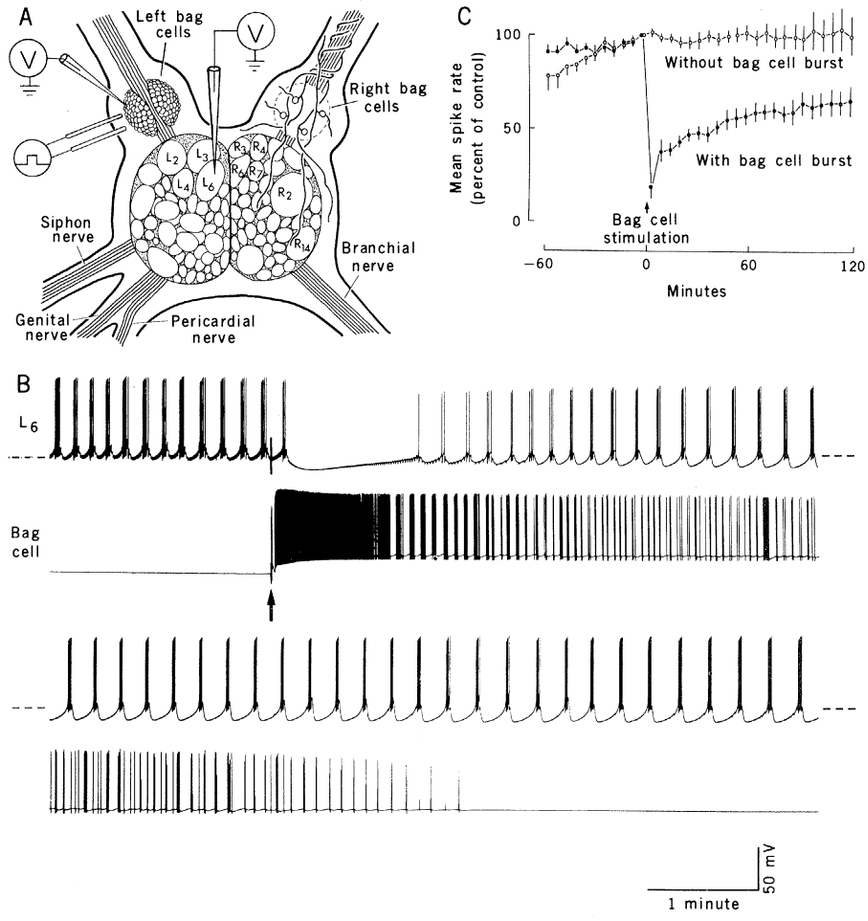

Fig. 1. Prolonged inhibition of a bursting pacemaker neuron after an electrically initiated discharge of neuroendocrine (bag) cell activity. (A) Schematic diagram of the dorsal surface of the abdominal ganglion, redrawn from (*12*), showing the locations of symmetrical left and right clusters of bag cells, identified neurons, and arrangement of stimulating and recording electrodes. A bipolar constant-current stimulating electrode was placed near the left (or right) bag cell cluster, while intracellular activity was simultaneously recorded from microelectrodes in a bag cell near the cathode of the stimulating electrodes and in a target neuron, L_3 or L_6. Some of the other identified ganglion neurons that also undergo prolonged inhibition after bag cell activation (*9*) are labeled. Four cells in the right cluster of bag cells are drawn schematically to show they send axonal processes into the sheath surrounding the ganglion. (B) Onset of prolonged inhibition of bursting pacemaker activity in target cell L_6 after an electrically activated bag cell discharge (arrow). The two upper traces are continued as the two lower traces. The dashed isopotential lines were added to delineate the amplitude of the underlying slow inhibitory potential (SIP) in the target cell. The SIP produced a decrease in the burst rate and the mean spike rate of the target cell. Spontaneously occurring inhibitory postsynaptic potentials from interneuron L_{10} can also be seen in the target cell recording; L_{10} is inhibited temporarily by bag cell activation (*9*). (C) Effect of stimulated bag cell activity on average spike rate of L_3 or L_6. In all experiments we used a uniform stimulation procedure that sometimes triggered a bag cell burst. When stimulation produced a bag cell burst, the data were included in one group (solid circles, $N = 8$); if stimulation failed to produce a bag cell burst, the data were included in another group (open circles, $N = 7$). For members of each group, mean spike rates for the 5.33-minute interval were normalized to the baseline control rate at minute 0, and the normalized values for each interval were averaged. The electrical stimulus was a train of ten 0.2-msec pulses applied at a rate of five per second. The stimulus intensity for each group was not significantly different (13.2 ± 2.8 versus 7.9 ± 2.3 mA). The evoked bag cell discharges lasted an average of 22 ± 3.2 minutes. This duration is the same as that recorded from intact animals at the initiation of egg laying (*1*, *10*).

tential was reduced from baseline values (Fig. 2C). This finding suggested that the reversal potential at the peak of the SIP was −84 mV, the membrane potential produced by the first step of the current pulse.

An alternative graphical representation of the same data is shown in Fig. 2D. Each line represents the steady-state current-voltage (I-V) characteristic of the membrane at the time a given three-step current pulse was delivered. The slope of the I-V line for the peak of the SIP was much smaller than the slope of the I-V line for the baseline period, which indicates that a large increase in membrane conductance had occurred. The relation between voltage and current was linear for each line; thus, the conductance increase was independent of voltage over the range of membrane potentials tested.

The baseline and peak conductance lines intersect at −84 mV, the reversal potential for the SIP. The mean value for eight reversal potentials measured by this method was −79 ± 1.6 mV [mean ± standard error of the mean [S.E.M.)]. The mean value is near −76 mV, the equilibrium potential for potassium ions (K^+) measured in these same neurons by Kunze and Brown (*15*) at the same temperature, measured with microelectrodes selective to K^+. The results therefore indicate that the peak of the SIP is associated with a membrane conductance increase to K^+.

At times later than the peak hyperpolarization of the SIP (the late phase of the response), the input conductance of the cell (and presumably the K^+ conductance) declined from its peak value but remained well above the baseline for the 45-minute duration of the experiment (Fig. 2C, lower panel) (*16*). Even though membrane conductance was relatively constant during the late phase, however, all three of the responses to imposed membrane current underwent hyperpolarizing shifts of approximately equal magnitude, suggesting that a second hyperpolarizing process was activated. This process was relatively independent of membrane conductance and occurred in addition to the maintained conductance increase to K^+. The second component was especially apparent in the membrane response to the first current step (−15 nA) (Fig. 2C); although the membrane potential was at the reversal potential for the early phase of the SIP, it began to shift in a negative direction 2 minutes after SIP onset, reaching a plateau at approximately 12 to 23 minutes. This hyperpolarizing process is also evident in Fig. 2D as the downward shift of the I-V lines at 23 and 46 minutes compared with the peak conductance line (*17*).

Three features of the SIP suggest that it is produced on or near the soma. (i) Hyperpolarization of the soma mem-

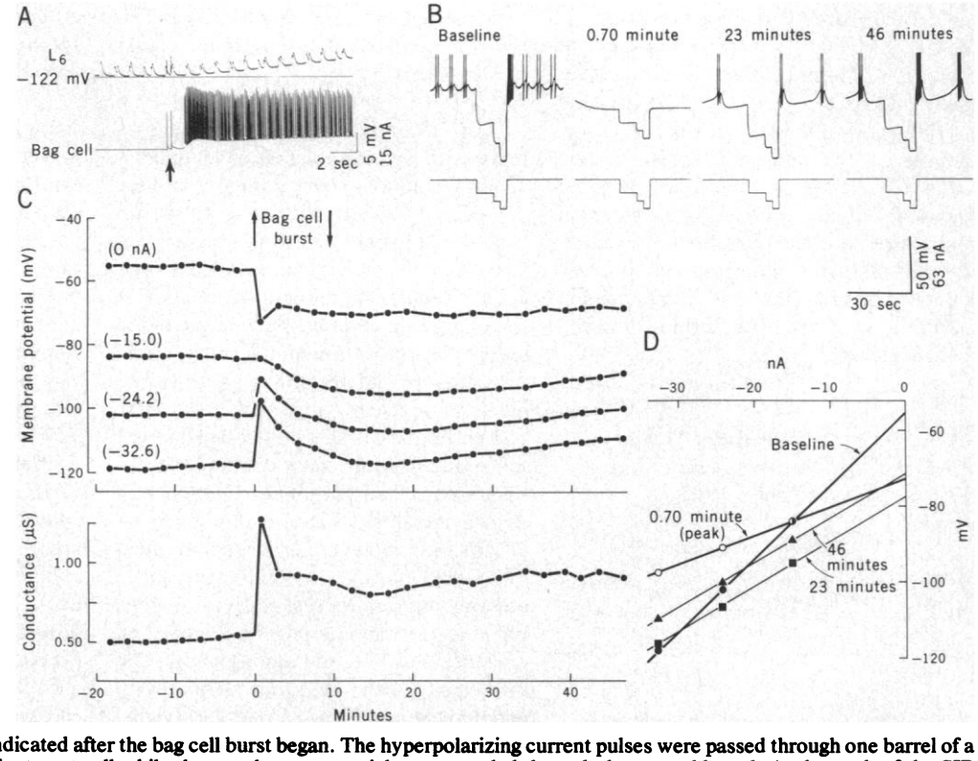

Fig. 2. Effect of membrane potential on the bag cell-induced SIP. (A) The onset of the SIP induced by bag cell activity was inverted to a depolarizing response when the membrane of the target cell was strongly hyperpolarized by constant current injection. The isopotential line (−122 mV) delineates the magnitude of the inverted response onset. There was no change in the pattern of spontaneously occurring synaptic potentials from interneuron L_{10} (evident as rapid upward deflections) that could account for the observed depolarization. The arrow indicates the time of bag cell stimulation (two 1.8-mA, 5-msec pulses). Delay to the onset of the response was approximately 1 second. (B to D) Effect of the membrane potential of the target cell on the SIP, as determined by periodic application of a three-step hyperpolarizing current pulse. Data are from a single experiment. (B) Examples of three-step current pulses (lower traces) and the membrane potential deflections (upper traces) they produced in target cell L_6 before (baseline) and at the various times indicated after the bag cell burst began. The hyperpolarizing current pulses were passed through one barrel of a double-barreled microelectrode in the target cell while the membrane potential was recorded through the second barrel. At the peak of the SIP (0.70 minute) and at later times, the membrane potential deflections produced by the second and third steps of current were smaller than those for baseline values, indicating a large, prolonged conductance increase associated with the SIP. (C) Upper panel: Effect of membrane potential on the magnitude and time course of the SIP. The uppermost trace represents the SIP produced in the unpolarized target cell by the bag cell burst discharge initiated at minute 0. The three lower traces show how the SIP is affected by increasing membrane hyperpolarization. At the peak of the SIP (0.70 minute), the reversal potential of the response was −84 mV, which is near the equilibrium potential for potassium ions. Later, a slow downward shift (seen most clearly in the three lower traces) indicates the presence of a second hyperpolarizing process superimposed on the maintained potassium conductance. The lower traces were constructed by applying a three-step hyperpolarizing current pulse to the target neuron at 2.33-minute intervals [examples are in (B)] and plotting the membrane potential obtained at the end of each step of current as a function of the time the pulse was applied. The uppermost trace was constructed by plotting the peak undershoot of the bursting pacemaker potential just before each three-step current pulse. Lower panel: Steady-state membrane conductance of the target cell, calculated from I-V lines as depicted in (D). (D) Changes in the steady-state current-voltage characteristic of the target cell membrane during the SIP. Each I-V line is constructed from the corresponding three-step pulse shown in (B). The I-V lines representing baseline and the peak SIP (0.70 minute) intersect at −84 mV, the reversal potential for the early phase of the SIP. During the late phase of the SIP, although membrane conductance was relatively constant, the I-V lines (23 and 46 minutes) shifted downward along the voltage axis compared with the peak conductance line, indicating the presence of the second hyperpolarizing process.

brane is maintained for the entire period in which mean spike rate and burst rate are decreased, and these effects on bursting pacemaker activity can be duplicated by direct hyperpolarization of the cell soma. (ii) The peak increase in conductance associated with the SIP is large, amounting to 61 ± 15 percent (N = 8) of the normal membrane conductance measured at the cell soma. Correspondingly, the somatic action potentials are partially shunted during the SIP (Fig. 1B). (iii) The reversal potential of the early phase of the SIP is near the equilibrium potential for K^+, as would be expected for a K^+ conductance increase located on or near the soma (*15*). These features of the SIP, and its smooth onset and prolonged duration, are consistent with the hypothesis that it is induced hormonally, rather than transynaptically, by a neurosecretory product released from bag cell axons in the sheath overlying the target cell somata.

The bag cells have two effects on bursting pacemaker neurons: inhibition, as described here, and augmentation, as described before (*7*). The question of how these multiple actions are mediated arises. Does one peptide, the egg-laying hormone, produce both of them or, among several alternatives, do the bag cells release more than one chemical messenger, each with its own effect on individual target neurons? Further studies addressing this question may provide new insights into the roles of peptides in naturally occurring interactions between neurons.

PHILIP BROWNELL
EARL MAYERI

Department of Physiology, School of Medicine, University of California, San Francisco 94143

References and Notes

1. I. Kupfermann, *Nature (London)* **216**, 814 (1967); *J. Neurophysiol.* **33**, 877 (1970).
2. F. Strumwasser, J. W. Jacklet, R. B. Alverez, *Comp. Biochem. Physiol.* **29**, 197 (1969).
3. R. E. Coggeshall, *J. Neurophysiol.* **30**, 1263 (1967).
4. W. T. Frazier, E. R. Kandel, I. Kupfermann, R. Waziri, R. E. Coggeshall, *ibid.*, p. 1288.
5. S. Arch, *J. Gen. Physiol.* **60**, 102 (1972); ———, T. Smock, P. Earley, *ibid.* **68**, 211 (1976); H. Gainer and Z. Wollberg, *J. Neurobiol.* **5**, 243 (1974); Y. P. Loh, Y. Sarne, H. Gainer, *J. Comp. Physiol.* **100**, 283 (1975); Y. P. Loh and H. Gainer, *Brain Res.* **92**, 181 (1975).
6. S. Arch, P. Earley, T. Smock, *J. Gen. Physiol.* **68**, 197 (1976); L. Toevs and R. Blackenbury, *Comp. Biochem. Physiol.* **29**, 207 (1969).
7. E. Mayeri and S. Simon, *Neurosci. Abstr.* **1**, 584 (1975); W. D. Branton, E. Mayeri, P. Brownell, S. B. Simon, *Nature (London)* **274**, 70 (1978).
8. W. D. Branton, S. Arch, T. Smock, E. Mayeri, *Proc. Natl. Acad. Sci. U.S.A.* **75**, 5732 (1978).
9. P. Brownell and E. Mayeri, *Neurosci. Abstr.* **3**, 173 (1977); E. Mayeri, P. Brownell, W. D. Branton, *J. Neurophysiol.*, in press.
10. H. M. Pinsker and F. E. Dudek, *Science* **197**, 490 (1977).
11. A bipolar stimulating electrode was placed (on the right or left bag cell cluster) such that the cathode was as close as possible to the bag cell being recorded. The bag cells were activated with rectangular, constant-current pulses (0.2 msec, 2 to 28 mA, delivered at a rate of five per second). The stimulus intensity was gradually increased until it produced subthreshold depolarizations in the recorded bag cell without evoking synaptic inputs to other ganglion neurons. The bag cell burst was then initiated by a 1- to 2-second train of these pulses.
12. I. Kupfermann and E. Kandel, *J. Neurophysiol.* **33**, 865 (1970).
13. It also shows that the delay to onset of the response is about 1 second. The estimated latencies in unpolarized cells are much longer, 4 to 8 seconds. This difference may be more apparent than real, however, since the bursting pacemaker potential in unpolarized cells obscures the precise onset of the SIP and produces larger estimates of onset delay.
14. In eight experiments, the mean time to peak was 0.92 ± 0.13 minute (± S.E.M.).
15. D. L. Kunze and A. M. Brown, *Nature (London) New Biol.* **229**, 229 (1971).
16. Input conductance was still 38 ± 7 percent (N = 4) above baseline 30 minutes after the onset of the response.
17. In four experiments, the amplitude of hyperpolarization attributable to the second process reached a maximum of 7.5 ± 1.4 mV at 18 ± 5.5 minutes after the beginning of the bag cell burst. In some examples, in which the second process was sufficiently dissociated from changes in input conductance, the downward shift of the I-V line was associated with a secondary hyperpolarization of the cell. In Fig. 1B, a secondary hyperpolarization started about 2 minutes after the onset of the bag cell discharge. It is possible that this is due to the onset of the second process.
18. We thank D. Branton, B. Rothman, M. J. Dennis, H. L. Fields, and J. I. Korenbrot for comments on an earlier version of this manuscript. Supported by A. P. Sloan and NIH postdoctoral fellowships to P.B. and PHS grant NS 10246 and NSF grant BNS 76-20978 to E.M.

5 September 1978; revised 6 November 1978

Immunocompetence in the Lowest Metazoan Phylum: Transplantation Immunity in Sponges

Abstract. *Isografts of* Callyspongia diffusa *fuse compatibly, but allografts are invariably incompatible. Extensive polymorphism of cell-surface histocompatibility markers is evident. The histocompatibility barriers range from strong to weak depending on the interclonal combination, but early rejection with conspicuous cytotoxic sequelae is typical. Reaction times of first-set, second-set, and third-party grafts indicate highly discriminating transplantation immunity with a specific memory component.*

Until recently, specific immune systems with selectively inducible responsiveness and a memory component were considered to be restricted to vertebrates. However, among higher invertebrates with diverse leukocyte-type cells, unequivocal immunorecognition at the allogeneic level has been reported in diverse worms (*1*), echinoderms (*2*), and tunicates (*3*). At the lower invertebrate level of coelenterates, allogeneic incompatibilities under controlled laboratory conditions are now documented for hydrozoans and gorgonians (*4*), as well as sea anemones (*5*) and corals (*6*). A specific alloimmune memory component of transplantation immunity has been demonstrated in representatives of three phylums: echinoderms, annelids, and coelenterates. To find among corals and now sponges the essential attributes of adaptive immunity (*7*) in a sharply discriminating form is surprising. Occurrence of specific allograft rejection at this lower level of phylogeny could represent the origins of both cell-mediated immunity and of the major histocompatibility complex of higher vertebrates.

Interspecific tissue incompatibility has long been known in sponges. When cell suspensions from two different species are mixed, each resulting aggregate appears to be composed of cells of one of the species alone (*8*). However, neither cell adhesion nor cell aggregation is strictly intraspecific among many sponges (*9*). Incompatibilities in mixed aggregation experiments do not usually lead to cell death, but this could reflect tests of insufficient duration (1 to 2 days) or loss of immunocytes during tissue disruption and cell processing. Several distinctive types of potential immunocytes known as amoebocytes, including some capable of efficiently phagocytosing foreign particles and cells, are found in intact sponges (*10*). Early interspecific rejection reactions have been observed in contact zones between intact branches of *Microciona* and *Haliclona*, but no incompatibility was discerned between allogeneic *Microciona* grafts in experiments of 3 weeks duration (*11*). The latter result in light of our findings is probably attributable to immunosuppression at low temperatures. Intraspecific incompatibility was first recorded among separate strains or individual sponges of the freshwater species, *Ephydatia fluviatilis*. Incompatibility in contact zones was manifest by a discrete border separating allogeneic sponges in contrast to control intrastrain grafts which fused or merged compatibly (*12*). No cytotoxic reactions or other sequelae of rejection were noted in conjunction with allogeneic nonfusion.

Colonies of the large, ramose species of the tropical Indo-Pacific sponge *Callyspongia diffusa* exist in several different locations in Kaneohe Bay, Hawaii. Fully viable *Callyspongia* exhibit a uniform

0036-8075/79/0427-0420$00.50/0